www.ietdl.org

Published in IET Microwaves, Antennas & Propagation
Received on 17th April 2010
Revised on 31st May 2011
doi: 10.1049/iet-map.2010.0154

ISSN 1751-8725

Mutual coupling suppression in microstrip array using defected ground structure

S. Xiao M.-C. Tang Y.-Y. Bai S. Gao B.-Z. Wang

Institute of Applied Physics, University of Electronic Science and Technology of China, Chengdu 610054, People's Republic of China
E-mail: xiaoshaoqiu@uestc.edu.cn

Abstract: A defected ground structure (DGS) is used to suppress mutual coupling between elements in a microstrip array and eliminate the scan blindness in an infinite phased array. Two kinds of DGSs, namely back-to-back U-shaped and dumbbell-shaped DGSs, are analysed and compared. The analysis indicates that the back-to-back U-shaped DGS is better at suppressing propagation of surface waves in microstrip substrate. A two-element microstrip array with back-to-back U-shaped DGS is designed and the array characteristics against different element distances are studied. The results show that the degree of the mutual coupling suppression is increased when the element distance is reduced. However, compared with the traditional array, a higher gain and lower side lobes are obtained when a larger element spacing is selected. The scan blindness of an infinite microstrip phased array in E-plane is studied by simulation, and the calculation demonstrates that the scan blindness can be eliminated by applying a back-to-back U-shaped DGS to the infinite phased array.

1 Introduction

In the design of microstrip arrays, mutual coupling between elements is an important factor to be considered. Many studies have indicated that the mutual coupling between elements can degrade seriously the performances of the array, leading to impedance mismatch, side-lobe level increases, scanning blindness occurrence and reduced gain [1]. Mutual coupling between microstrip elements is caused by both space waves and surface waves. A surface wave has a significant impact on the mutual coupling when the thickness h of the microstrip substrate is greater than $0.3\lambda_0/(2\pi/\sqrt{\varepsilon_r})$ [2], where λ_0 is the operating wavelength in free space and ε_r is the relative permittivity of the substrate. In the past decades, many methods have been developed to reduce the mutual coupling caused by surface waves between antenna elements in the design of microstrip arrays. In [3–5], shorted patches were proposed to prevent excitation of the surface wave mode. In [6–8], electromagnetic bandgap (EBG) structures were used to suppress mutual coupling. An EBG structure creates a so-called electromagnetic crystal to suppress surface-wave propagation, and thus, unwanted mutual coupling between elements is decreased.

Recently, defected ground structures (DGS), which are formed by etching patterns on the ground plane, have received much attention. As a resonator, the DGS is a compact structure. This advantage has resulted in its various applications, such as microwave filters and matching circuits as well as suppressing harmonic and cross-polarisation in microstrip antennas [9–14]. However, there are only a limited number of results published concerning the suppression of mutual coupling between elements in antenna arrays [15]. Compared with EBG structures, the advantage of DGS is that it can realise bandgap effect with a more compact circuit size.

Here, the mutual coupling suppression in microstrip arrays is studied by using DGS. Single U-shaped, dumbbell-shaped and back-to-back U-shaped DGS, shown in Figs. 1*b–d*, respectively, are analysed and compared. The back-to-back U-shaped DGS is adopted to upgrade the performance of microstrip phased arrays by suppressing mutual coupling between antenna elements.

2 Characteristic analysis of DGS

Numerical simulation, performed with the commercial software Ansoft HFSS 9.2, is used to predict the bandgap of the DGS. DGSs are etched on the ground plane between elements in the microstrip array when they are applied to suppress the mutual coupling of the elements. In order to test its performance, the DGS is laid on the centre of the ground plane between two weakly coupled microstrip lines with 50 Ω characteristic impedance, as shown in Fig. 1*a*. The scattering parameter S_{21} between two microstrip line ports is calculated to study the resonance characteristic of the DGS. This method has been successfully used in ultra-wideband filter design to study the property of the microstrip stepped-impedance resonators [16–18].

First, a single U-shaped DGS in Fig. 1*b* is designed to support a bandgap around 6 GHz. The available microstrip substrate has a relative permittivity of 10.2 and a thickness of 2 mm ($>0.3\lambda_0/(2\pi/\sqrt{\varepsilon_r})$). A pronounced surface wave can be excited in this substrate. The dimension of the single

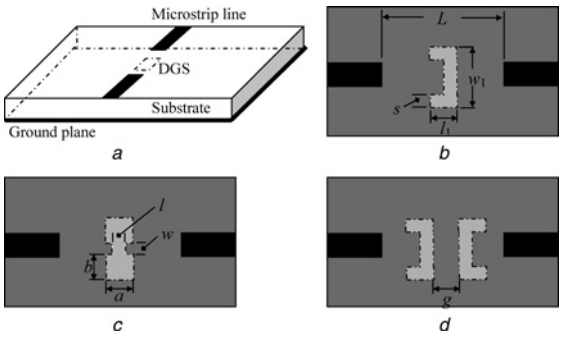

Fig. 1 *Configurations of the DGSs*

a 3-D view of DGS with two weakly coupled microstrip line
b Single U-shaped DGS
c Dumbbell-shaped DGS
d Back-to-back U-shaped DGS

U-shaped DGS is optimised to obtain a wider bandgap characteristic and the design parameters are $l_1 = 3.3$ mm, $w_1 = 7.4$ mm and $s = 1.4$ mm. For comparison, the dumbbell-shaped DGS in Fig. 1*c* is designed with the same bandgap, and the optimised parameters are $a = 3.6$ mm, $b = 4$ mm, $w = 0.9$ mm and $l = 1.8$ mm. The simulated S_{21} are shown in Fig. 2. As a reference, the simulated result for the structure without DGS is also shown in Fig. 2. In our studies, the distance L between two open ports of the weakly coupled microstrip lines is 20 mm, which is enough to avoid a strong coupling between DGS and the open microstrip lines.

For evaluating the performance of the DGS, the rejection bandwidth is defined covering a frequency range in which S_{21} is suppressed by more than 3 dB compared with that of the structure without DGS. From Fig. 2, it can be seen that the two DGSs have the similar bandgap characteristics, that is, a fractional rejection bandwidth of about 3.5% at a frequency of about 6 GHz. However, the area of the etched aperture is reduced from $2ab + wl = 30.4\ \text{mm}^2$ for the conventional dumbbell-shaped DGS to $2sl_1 + s(w_1 - 2s) = 14.9\ \text{mm}^2$ for the U-shaped one.

Multiple circuit units are usually cascaded for increasing the stopband in bandstop filter design [19]. Considering the symmetry and the trade-off between compact structure and rejection bandwidth, here, two back-to-back U-shaped DGS units are cascaded for extending the rejection bandwidth, as shown in Fig. 1*d*. The optimised distance between the two back-to-back U-shaped DGS units is $g = 4.5$ mm. The

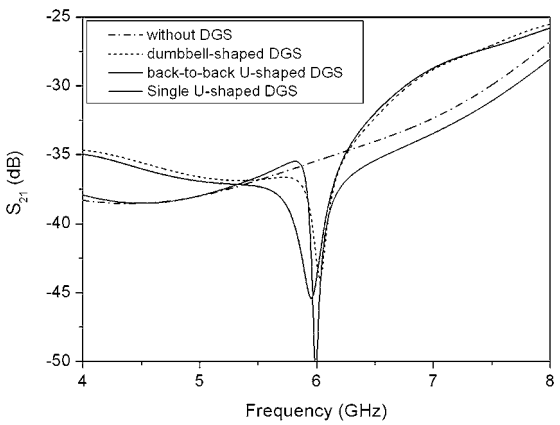

Fig. 2 *Simulated S_{21} with and without DGS between two weakly coupled microstrip line ports*

parameter S_{21} is simulated and shown in Fig. 2. As illustrated, this DGS shows a rejection band from 5.76 to 6.15 GHz (a fractional bandwidth of 7%) and twice the enhancement of the rejection bandwidth is achieved compared with that of single-unit one. Meanwhile, the area of the etched aperture (29.8 mm^2, twice the area for the U-shaped DGS) is still less than that of single dumbbell-shaped DGS.

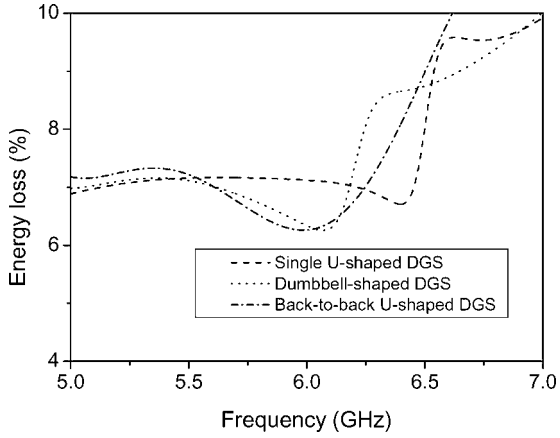

Fig. 3 *Energy loss for different DGSs*

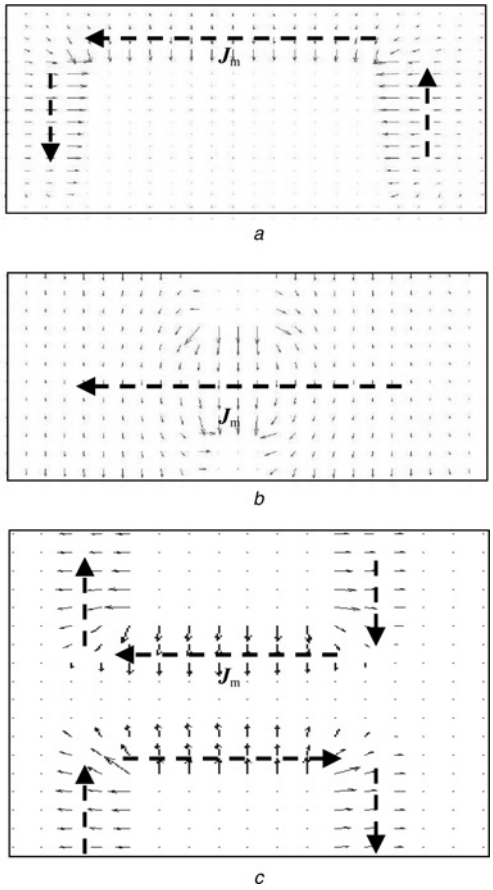

Fig. 4 *Electric field distributions in DGS aperture, fine lines denote electric fields and thick dashed lines denote equivalent magnetic current*

a Single U-shaped DGS
b Dumbbell-shaped DGS
c Back-to-back U-shaped DGS

The energy loss resulting from different DGSs is also compared. The energy loss is scaled by the expression

$$\mathrm{EL}(\%) = [1 - (|S_{11}|^2 + |S_{21}|^2)] \times 100\% \quad (1)$$

Fig. 3 shows the calculated results. The back-to-back U-shaped DGS exhibits a lower energy loss within a wider band. This is explored by observing the electric field distributions. The tangential electric fields in the etched DGS apertures are shown in Fig. 4. Based on the equivalence principle, the tangential electric field $\boldsymbol{E}_t$ can radiate energy as an equivalent magnetic current

$$\boldsymbol{J}_m = \boldsymbol{E}_t \times \hat{\boldsymbol{n}} \quad (2)$$

where $\hat{\boldsymbol{n}}$ is the normal vector of the ground plane. From Fig. 4, it is seen that the electric field distribution in the back-to-back U-shaped DGS has the property of reverse symmetry, which can result in a weaker radiation compared with other structures according to the superposition principle. It implies that the back-to-back U-shaped DGS can induce a weaker radiation loss.

3 Two-element array with back-to-back U-shaped DGS

Previous studies indicated that the mutual coupling between E-plane-coupled elements is stronger than that between H-plane-coupled elements because the stronger surface wave is excited along the E-plane [20–22]. Therefore only the mutual coupling suppression between the E-plan-coupled elements has been studied to validate the performance of the DGS.

A coaxial-line-fed E-plane-coupled two-element microstrip array, supported on a substrate with a thickness of 2.0 mm and relative permittivity of 10.2, is designed at 6 GHz (the fundamental operating frequency). The top and side views of the array are shown in Figs. 5*a* and *b*, respectively. The radiation patches have the same size of $W_p \times L_p = 6.7$ mm $\times$ 6.6 mm. The feed position is $L_f = 2.8$ mm. A finite ground plate with a size of $L_{gg} =$ 140 mm $\times$ 70 mm is used.

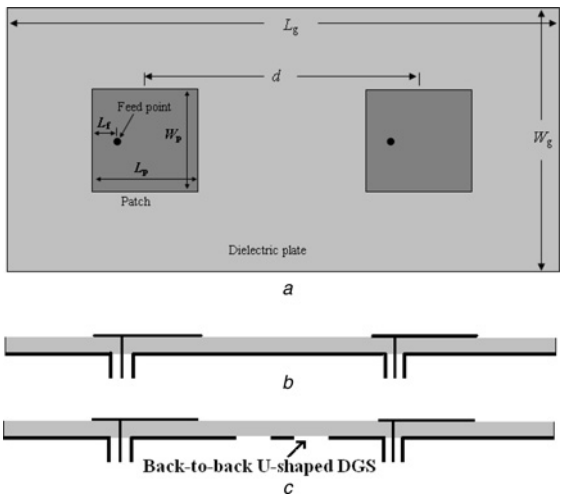

Fig. 5 *Configurations of microstrip arrays*

a Top view
b Side view of traditional array
c Side view of array with back-to-back U-shaped DGS

Based on [20, 21], in microstrip arrays the mutual coupling between elements results mainly from surface waves when the distance d between adjacent elements is larger than $0.3\lambda_0$. Here, arrays with distance variation from $0.5\lambda_0$ to λ_0 are studied. In order to achieve a significant low level of mutual coupling, the back-to-back U-shaped DGS is etched at the centre of the ground plate between antenna elements. The side view of the array is shown in Fig. 5*c*.

Fig. 6*a* shows the calculated S_{21} (mutual coupling) against element distances when the array is loaded by DGS and no DGS. The calculated results indicate that the mutual coupling between two antenna ports is suppressed effectively by using the back-to-back U-shaped DGS;

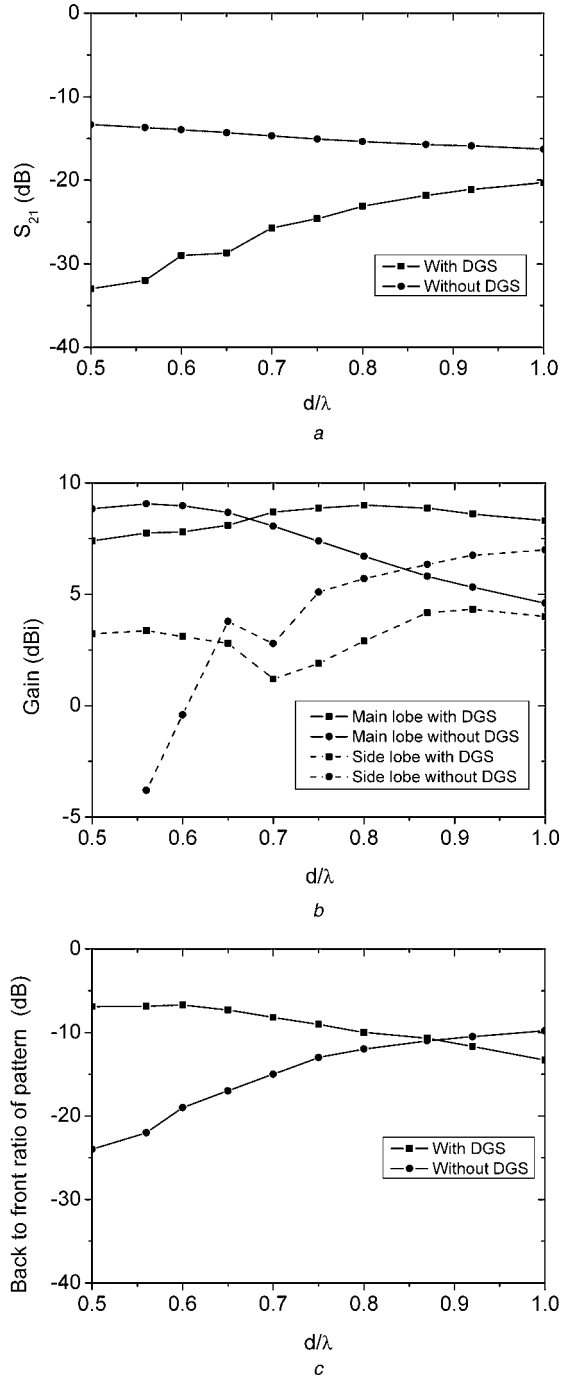

Fig. 6 *Calculated array performance against element distance*

a S_{21}
b Main-lobe gain and side-lobe gain
c Back-to-front ratio of pattern

doi: 10.1049/iet-map.2010.0154

meanwhile, the degree of the mutual coupling suppression is reduced with the increase of the element distance. The change rule of the mutual coupling suppression may be analysed qualitatively. Because of the dispersive propagation of the surface wave, the shorter the distance away from the antenna, the stronger the surface wave is. Thus, the mutual coupling suppression is reduced with the increasing of the element distance, because the energy intercepted by the DGS is lower when the element distance is larger.

Fig. 6*b* shows the calculated main lobe and side-lobe gains (i.e. the peak gains for main and side lobes) against array distances when the array is loaded by DGS and no DGS. Fig. 6*c* demonstrates the back to front ratio of the radiation patterns for two cases. As shown in Fig. 6*b*, the main-lobe gain of the array without DGS reduces with increasing element distance, and the reduction is due to the higher side lobes and the mutual coupling between array elements. The higher side lobes arise from the larger array spacing. The side-lobe level is higher than the main-lobe level when the array has a larger element distance. Fig. 6*c* shows that the higher back-direction radiation is generated in the array with the DGS when the element distance is smaller because the stronger surface wave energy is intercepted and leaked by the DGS. The gain of the array with DGS is then lower when the element distance is smaller (less than $0.67\lambda_0$ in this example), compared with the array without DGS. However, the gain is higher than that of the array without DGS when the element distance is larger than $0.67\lambda_0$. This result can also be explained qualitatively. The influence on the gain of the array with DGS includes mainly two parts. One part is the back-direction radiation through the DGS aperture; the other part is the surface wave reflected into antenna elements by DGS. They can reduce and enhance the array gain, respectively. When the contribution of the former is dominant the gain is reduced, meanwhile, the gain is improved if the latter is dominant. It must be mentioned that the mutual coupling (between elements suppressed by DGS) is extremely low, as shown in Fig. 6. Thus, it hardly influences the array gain. Another important advantage of the array with DGS is that the gain and side-lobe level are more stable even if the element distance changes from $0.5\lambda_0$ to λ_0. Cavity-backed structures could be used to suppress the back-direction radiation and further improve the array performance based on the method in [17].

In order to validate the studied results, arrays with element distances of $d = 43.5$ mm and $d = 28.0$ mm are fabricated and measured to demonstrate the performance of the DGS. For the purpose of comparison, traditional arrays (the ones without DGS) are also measured. All the measured scattering parameters are shown in Fig. 7. The experiments indicate that the DGS results in a strong mutual coupling reduction (i.e. the difference between the mutual coupling (S_{21}) in the array with DGS (in Fig. 5*c*) and that in the traditional array (in Fig. 5*b*) of 7.2 dB when $d = 43.5$ mm, and 15.1 dB when $d = 28.0$ mm at each central operating

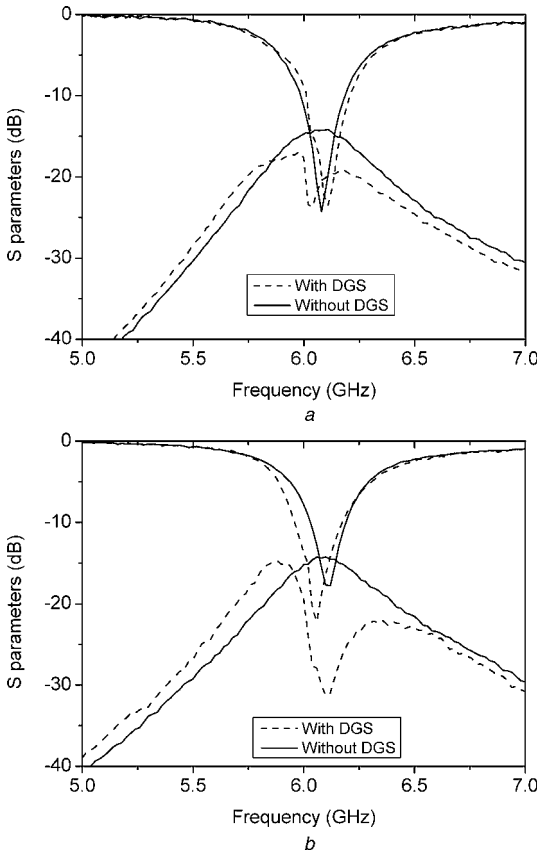

Fig. 7 *Measured S parameters of array with and without back-to-back U-shaped DGS*

a $d = 43.5$ mm
b $d = 28.0$ mm

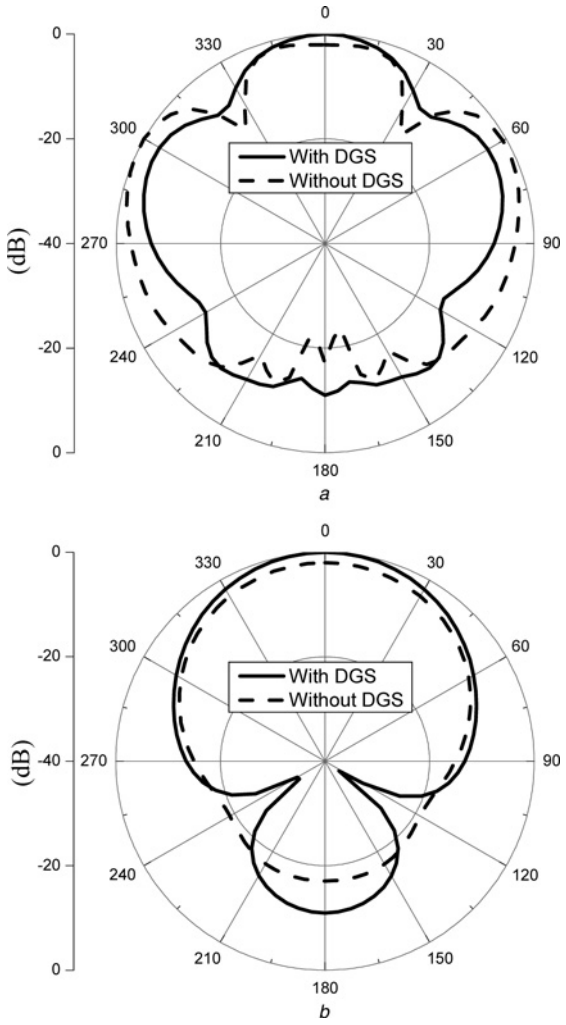

Fig. 8 *Measured radiation patterns of array with and without back-to-back U-shaped DGS when d = 43.5 mm*

a E-plane
b H-plane

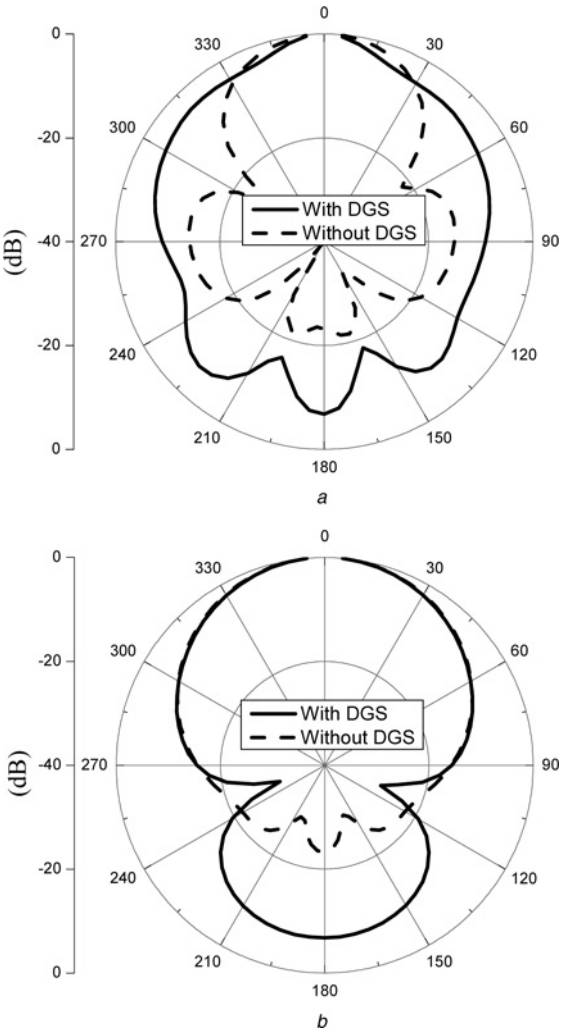

Fig. 9 *Measured radiation patterns of array with and without back-to-back U-shaped DGS when d = 28.0 mm*

a E-plane
b H-plane

frequencies around 6.03 GHz. To measure the radiation patterns of the arrays, a power divider is used to feed the antenna elements with in-phase. The measured radiation patterns at the operation frequency are shown in Figs. 8 and 9. A good agreement between experimental and analysed results is observed.

It is well known that due to pronounced surface wave excitation, the strong mutual coupling could worsen radiation performance of the array [23] shown in Fig. 8*a*, which leads to ripple in the radiation pattern. Since the mutual coupling is suppressed by DGS, strong nulls disappearance and side-lobes degradation are observed. The reason is that as the distance becomes larger, the mutual coupling degrades. Moreover, because of the larger distance, the proposed DGS performance (in Fig. 8*a*) for mutual coupling suppression is not as good as that in Fig. 9*a*. The comparison results are in accordance with the result in Figs. 6*a* and *c*, respectively.

4 Scan blindness elimination in infinite microstrip phased array

The scan characteristic of the infinite microstrip phased array with the back-to-back U-shaped DGS is studied. Fig. 10 shows the infinite phased array. In this array, the DGS are only arranged for E-plane mutual coupling reduction. The periods of the elements along the *x*- and *y*-axis are the same. Based on Floquent's theorem, the scan characteristic of the array can be extracted by analysing one of the elements in the array [24, 25]. Ansoft HFSS 9.2 is used to perform this simulation. Periodic boundary conditions, called master and slave boundaries in Ansoft HFSS, are applied to the simulated unit cell in the *x*-direction and a *y*-direction, and a perfectly matched layer is applied in the *z*-direction.

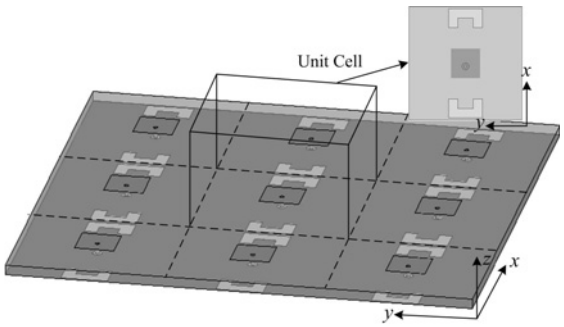

Fig. 10 *Infinite phased array when back-to-back U-shaped DGS is used to suppress the mutual coupling between the E-plane-coupled elements*

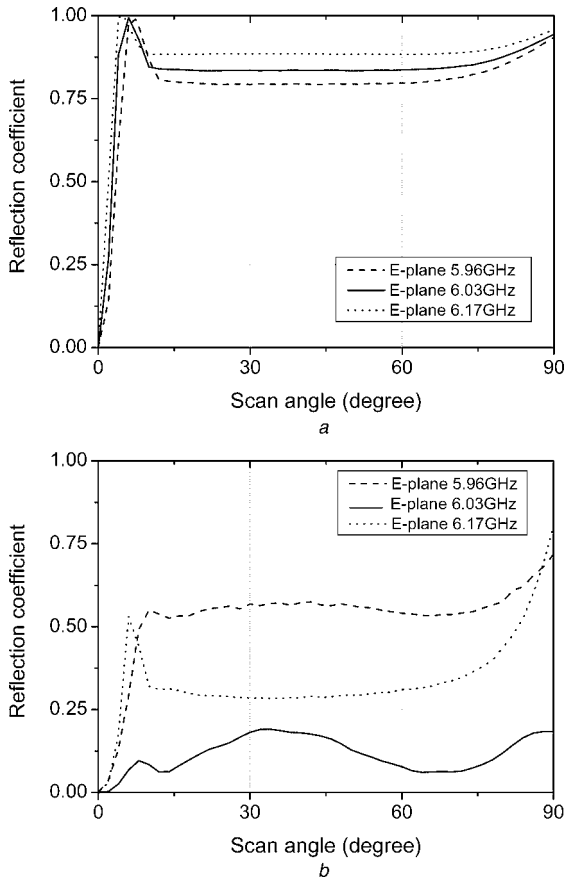

Fig. 11 *Magnitudes of array reflection coefficient against the scan angle in E-plane over the operation frequency band when d = 43.5 mm*

a Without DGS
b With DGS

doi: 10.1049/iet-map.2010.0154

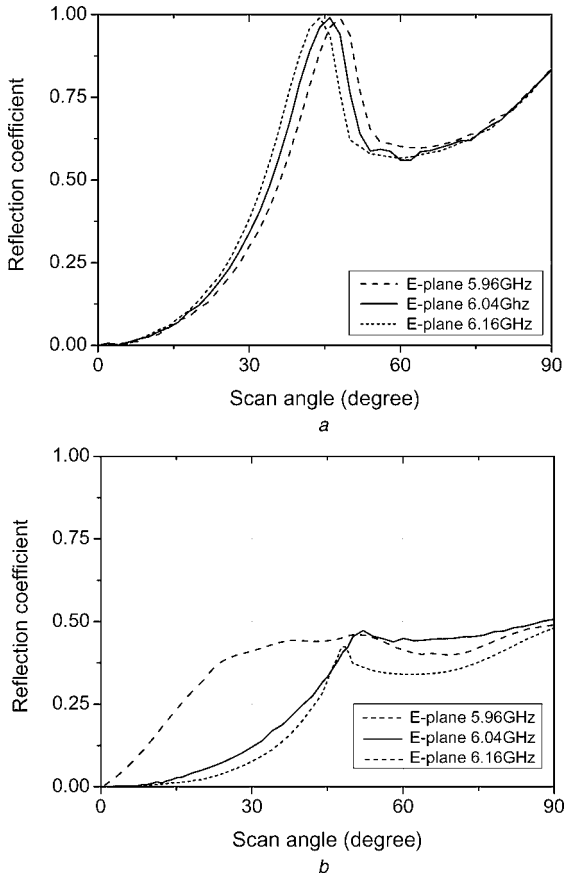

Fig. 12 *Magnitudes of array reflection coefficient against the scan angle in E-plane over the operation frequency band when $d = 28.0$ mm*

a Without DGS
b With DGS

The active reflection coefficient of the array is used to describe the array scan characteristic and is defined as

$$|R| = \frac{Z_{in}(\theta, \varphi) - Z_{in}(0, 0)}{Z_{in}(\theta, \varphi) + Z_{in}^{*}(0, 0)} \tag{3}$$

where $Z_{in}(\theta, \varphi)$ is the input impedance of the element when the array scans its main beam to (θ, φ), and $Z_{in}^{*}(0, 0)$ is the conjugate of $Z_{in}(0, 0)$. To be matched to the feedline at broadside, we should have $Z_{in}(0, 0)$ equal to the characteristic impedance of the feedline. In this study, φ is fixed to zero because we only study the array scan characteristic in the E-plane.

Figs. 11 and 12 give the calculated active reflection coefficient of the infinite phased array without and with the back-to-back U-shaped DGS at the lowest frequency, the centre frequency and the highest frequency of the operation frequency band that is determined with a criterion of the reflection coefficient. Figs. 11*a* and 12*a* demonstrate that, for the traditional phased array, scan blindness occurs in the E-plane ($\phi = 0^{\circ}$) at an angle of about $\phi = 6^{\circ}$ and $\phi = 48^{\circ}$ when $d = 43.5$ mm and $d = 28.0$ mm, respectively. Just as shown in Figs. 12*b* and *c*, when the DGS is loaded between adjacent E-plane-coupled elements to suppress element mutual coupling, the scan blindness is eliminated strongly in both arrays. Comparing Fig. 11*b* with Fig. 12*b*, it is found that a better performance in scan blindness

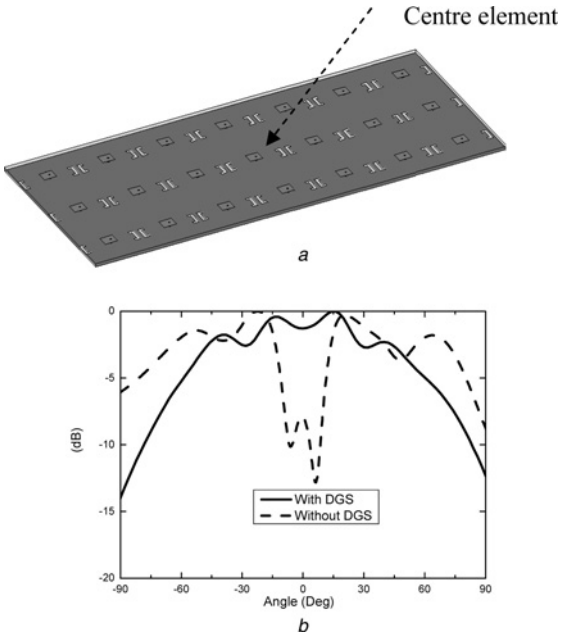

Fig. 13 *Typical centre active pattern of 7 × 3 element array*

a Configuration
b Patterns in E-plane

elimination is achieved by the array with $d = 28.0$ mm owing to the stronger mutual coupling suppression ability.

Furthermore, a typical centre active pattern of 7 × 3 element array with an interelement space of 43.5 mm is also studied, and the scheme is shown in Fig. 13*a*. Fig. 13*b* shows that there are two symmetrically significant nulls at $\pm 6^{\circ}$ in the normalised gain pattern of the centre active element in the array without DGSs and the positions of two nulls is in accordance with the scan blindness positions in Fig. 11*a* [23]. By comparison, the nulls vanish and the main lobe becomes smoother due to the mutual coupling reduction by DGSs.

5 Conclusion

In this paper, a simple and compact DGS, consisting of two back-to-back U-shaped DGS units, is used to suppress mutual coupling between E-plane-coupled microstrip antenna elements. The proposed back-to-back U-shaped DGS can provide good bandgap characteristics with a smaller etched aperture area. Two-element microstrip arrays with back-to-back U-shaped DGS are studied and the array characteristics against different element distances are explored. The studies indicate that, compared with the traditional array, the mutual coupling in the array loaded by DGS is suppressed effectively, and the new array has a better performance, such as stable main-lobe gain and a lower side-lobe level. The scanning blindness elimination is observed in infinite microstrip phased arrays due to application of DGSs.

6 Acknowledgment

This work was in part supported by the Hi-Tech Research and Development Program of China under grant 2009AA01Z231, in part by the New-century Talent Program of the Education Department of China under grant NCET070154, in part by the Foundation of State Key Laboratory of Millimeter Waves under grant no. K200809 and in part by the National

Natural Science Foundation of China under grants no. 60872034 and 60971029.

7 References

1 Pozar, D.M., Schaubert, D.H.: 'Analysis of an infinite array of rectangular microstrip patches with idealized probes feeds', *IEEE Trans. Antennas Propag.*, 1984, **32**, (10), pp. 1101–1107

2 James, J.R., Henderson, A.: 'High-frequency behavior of microstrip open-circuit terminations', *IEE J. Microw. Opt. Acoust.*, 1979, **3**, (9), pp. 205–218

3 Amendola, G., Boccia, L., Massa, G.: 'Shorted elliptical patch antennas with reduced surface waves on two frequency bands', *IEEE Trans. Antennas Propag.*, 2005, **53**, (6), pp. 1946–1956

4 Jackson, D.R., Williams, J.T., Bhattacharyya, A.K., Smith, R.L., Buchheit, S.J., Long, S.A.: 'Microstrip patch designs that do not excite surface waves', *IEEE Trans. Antennas Propag.*, 1993, **41**, (8), pp. 1026–1037

5 Khayat, M.A., Chen, R.L., Jackson, D.R., Williams, J.F.: 'Mutual coupling between reduced surface-wave microstrip antennas', *IEEE Trans. Antennas Propag.*, 2000, **48**, (10), pp. 1581–1593

6 Ramon, G., Maagt, P., Sorolla, M.: 'Enhanced patch-antenna performance by suppression surface waves using photonic-bandgap substrates', *IEEE Trans. Microw. Theory Tech.*, 1999, **47**, (11), pp. 2131–2138

7 Yang, H.-Y., Alexopoulos, N.G., Yablonovitch, E.: 'Photonic band-gap materials for high-gain printed circuit antennas', *IEEE Trans. Antennas Propag.*, 1997, **45**, (1), pp. 185–187

8 Yang, L., Fan, M.Y., Chen, F.L., She, J.Z., Feng, Z.H.: 'A novel compact electromagnetic bandgap structure and its applications for microwave circuits', *IEEE Trans. Microw. Theory Tech.*, 2005, **53**, (1), pp. 183–190

9 Rahman, A.B., Verma, A.K., Boutejdar, A., Omar, A.S.: 'Control of bandstop response of Hi-Lo microstrip low-pass filter using slot in ground plane', *IEEE Trans. Antenna Propag.*, 1997, **45**, (1), pp. 185–187

10 Choi, H.-J., Lim, J.-S., Jeong, Y.-C.: 'A new design of Doherty amplifiers using defected ground structure', *IEEE Microw. Compon. Lett.*, 2006, **16**, (12), pp. 687–689

11 Liu, H., Li, Z., Sun, X., Mao, J.: 'Harmonic suppression with photonic bandgap and defected ground structure for a microstrip patch antenna', *IEEE Microw. Compon. Lett.*, 2005, **15**, (2), pp. 55–56

12 Guha, D., Biswas, M., Antar, Y.M.M.: 'Microstrip patch antenna with defected ground structure for cross polarization suppression', *IEEE Antennas Wirel. Propag. Lett.*, 2005, **4**, pp. 455–458

13 Ting, S.-W., Tam, K.-W., Martins, R.P.: 'Miniaturized microstrip lowpass filter with wide stopband using double equilateral U-shaped defected ground structure', *IEEE Microw. Compon. Lett.*, 2006, **16**, (5), pp. 240–242

14 Guha, D., Biswas, S., Biswas, M., Siddiqui, J.Y., Antar, Y.M.M.: 'Concentric ring-shaped defected ground structures for microstrip applications', *IEEE Antennas Wirel. Propag. Lett.*, 2006, **5**, (1), pp. 402–405

15 Guha, D., Biswas, S., Joseph, T., Sebastian, M.T.: 'Defected ground structure to reduce mutual coupling between cylindrical dielectric resonator antennas', *Electron. Lett.*, 2008, **44**, (14), pp. 836–837

16 Zhu, L., Sun, S., Menzel, W.: 'Ultra-wideband (UWB) bandpass filters using multiple-mode resonator', *IEEE Microw. Wirel. Compon. Lett.*, 2005, **15**, (11), pp. 796–798

17 Zhu, L., Tan, B.C., Quek, S.J.: 'Miniaturized dual-mode bandpass filter using inductively loaded cross-slotted patch resonator', *IEEE Microw. Wirel. Compon. Lett.*, 2005, **15**, (1), pp. 22–24

18 Li, R., Zhu, L.: 'Compact UWB bandpass filter using stub-loaded multiple-mode resonator', *IEEE Microw. Wirel. Compon. Lett.*, 2007, **17**, (1), pp. 40–42

19 Hong, J.S., Lancaster, M.J.: 'Microwave filters for RF/microwave application' (Wiley, New York, 2001)

20 Yang, F., Rahmat-Samii, Y.: 'Microstrip antennas integrated with electromagnetic band-gap (EBG) structures: a low mutual coupling design for array applications', *IEEE Trans. Antennas Propag.*, 2003, **51**, (10), pp. 2936–2945

21 Mohammadian, A.H., Martin, N.M., Griffin, D.W.: 'A theoretical and experimental study of mutual coupling in microstrip antenna arrays', *IEEE Trans. Antennas Propag.*, 1989, **37**, (10), pp. 1217–1223

22 Jedlicka, R.P., Poe, M.T., Carver, K.R.: 'Measured mutual coupling between microstrip antennas', *IEEE Trans. Antennas Propag.*, 1981, **29**, (1), pp. 147–149

23 Iluz, Z., Shvit, R., Bauer, R.: 'Microstrip antenna phased array with electromagnetic bandgap substrate', *IEEE Trans. Antennas Propag.*, 2004, **52**, (6), pp. 1446–1453

24 Diamond, B.L.: 'Small arrays-their analysis and their use for the design of array elements', in Oliner, A.A., Knittel, G.H. (Eds.): 'Phased array antennas' (Artech House, Norwood, MA, 1972), pp. 127–131

25 Pozar, D.M.: 'Analysis of an infinite phased array of aperture coupled microstrip patches', *IEEE Trans. Antennas Propag.*, 1989, **37**, (4), pp. 418–425

doi: 10.1049/iet-map.2010.0154